Kinetic Isotope Effects as Probes of the Mechanism of Galactose Oxidase†

Mei M. Whittaker,‡ David P. Ballou,§ and James W. Whittaker*,‡

Department of Biochemistry and Molecular Biology, Oregon Graduate Institute of Science and Technology, P.O. Box 91000, Portland, Oregon 97291-1000, and Department of Biological Chemistry, University of Michigan Medical School, Ann Arbor, Michigan 48109-0606

Received February 10, 1998

ABSTRACT: Galactose oxidase (GO) is a member of the family of radical-coupled copper oxidases, enzymes containing a free radical coordinated to copper in the active site. In catalysis GO cycles between an oxidized state (comprising Cu(II) with a unique cysteinyl-tyrosine radical) and a reduced state (comprising Cu(I) with the singlet cysteinyl-tyrosine) as it catalyzes the two-electron oxidation of alcohols to aldehydes and the subsequent reduction of O_2 to H_2O_2. A ping-pong mechanism involving radical intermediates has been proposed for GO catalysis. Previous steady-state kinetics studies have demonstrated a KIE of 7−8 that was attributed to substrate oxidation, a process involving the stereospecific abstraction of the *pro*-S hydrogen from the 6-hydroxymethyl group of galactose. We have used rapid kinetics methods to measure the anaerobic reduction of GO substrate at 4 °C and carry out enzyme-monitored turnover experiments using 6-protio and 6-deutero substrates, both in H_2O and D_2O. At concentrations below K_m, the apparent second-order rate constant for protio-substrate oxidation, k_{red}, was 1.59×10^4 M^{-1} s^{-1}, while that for deuterated substrate was 7.50×10^2 M^{-1} s^{-1}, a KIE of 21.2. Steady-state measurements of oxygen consumption at low galactose concentrations reveal an unusually large isotope effect ($k_H/k_D = 22.5 \pm 2$) for oxidation of 1-*O*-methyl-6,6′-di-[^{2}H]-α-D-galactopyranoside, and at high galactose concentrations, where the oxygen half-reaction is rate-limiting in catalysis, a surprisingly large KIE ($k_H/k_D = 8 \pm 1$) for the reduction of O_2 to H_2O_2. There is no detectable solvent isotope effect (<5%) on any of these measurements. This shows that there are no exchangeable protons involved in any kinetically significant step and that the hydrogen atom removed from galactose is not lost to solvent during catalysis; instead, it also participates in the rate-limiting step of the subsequent reaction with oxygen. At concentrations below K_m, apparent second-order rate constants for protio-substrate oxidation ($k_{red} = 1.5 \times 10^4$ M^{-1} s^{-1}) and O_2 reduction ($k_{ox} = 8 \times 10^6$ M^{-1} s^{-1}) have been estimated from measurements both by steady-state oxygen electrode and by enzyme-monitored turnover. This is completely consistent with the anaerobic studies mentioned above. Our results show that the enzyme is essentially fully oxidized while in steady-state turnover, consistent with the reduction step being nearly fully rate-limiting at practical substrate concentrations, due to the very fast reaction with physiological concentrations of O_2. Overall, the catalytic reaction is in concordance with a ping-pong mechanism. The large KIE associated with reduction of the enzyme in all three methods appears to reflect hydrogen atom radical abstraction by the active site tyrosine radical in the rate-determining step, in agreement with the previously proposed radical mechanism for GO. The KIE determined at low substrate concentrations (where oxidation of substrate is rate determining) from steady-state oxygen consumption measurements, varies from 22.5 at 4 °C to 13 at 45 °C, consistent with tunneling being involved in the hydrogen atom transfer step.

Galactose oxidase is the most extensively studied of a recently recognized family of redox metalloenzymes, the radical copper oxidases (*1*), that are found in fungi [galactose oxidase (*2*,*3*), glyoxal oxidase (*4*,*5*)] and prokaryotes [where a structural homolog, the FbfB protein (*6*), has recently been reported]. One of the remarkable features of these enzymes is the presence of an unusually stable tyrosine free radical which is coordinated to the copper and imparts to this center its distinctive optical and EPR spectra (*1*,*7*). The overall reaction catalyzed by GO[1] involves transfer of the equivalent of dihydrogen from simple alcohols to dioxygen to form hydrogen peroxide and the product aldehyde (eq 1).

$$RCH_2OH + O_2 \rightarrow RCHO + H_2O_2 \qquad (1)$$

Biologically, the H_2O_2 produced by the radical copper oxidases is thought to serve variously as a bacteriostatic agent or as the essential cosubstrate for peroxidases (*1*). Galactose

† Support for this project from the National Institutes of Health (GM 46749 to J.W.W., and GM 20877 to D.P.B.) is gratefully acknowledged.

* Author to whom correspondence should be addressed. Telephone: 503-690-1065. FAX: 503-690-1464. E-mail: jim@bmb.ogi.edu.

‡ Oregon Graduate Institute of Science and Technology.

§ University of Michigan Medical School.

[1] Abbreviations: GO, galactose oxidase; AGO, active galactose oxidase; IAGO, reductively inactivated form of galactose oxidase containing Cu(II) but no free radical; RGO, reduced Cu(I)-containing galactose oxidase; [H_2]-gal, 1-*O*-methyl-6,6′-di[^{1}H]-α-D-galactopyranoside; [D_2]-gal, 1-*O*-methyl-6,6′-di[^{2}H]-α-D-galactopyranoside; KIE, kinetic isotope effect for deuterated substrate.

S0006-2960(98)00328-6 CCC: $15.00
Published on Web 05/12/1998

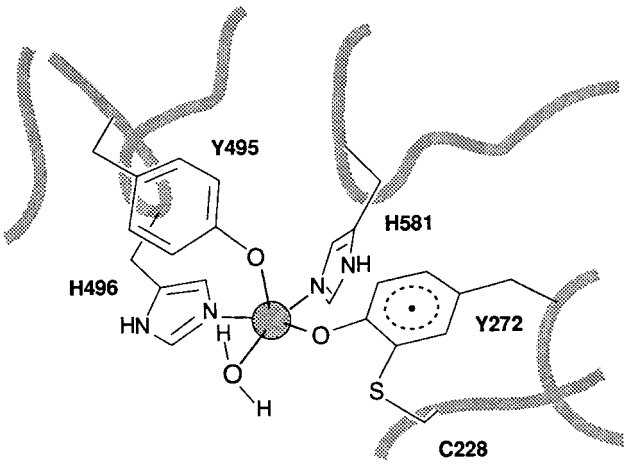

FIGURE 1: The active site of galactose oxidase. (Based on crystallographic coordinates from PDB ID 1GOG, see refs *14*, *15*).

and 1-*O*-methyl-6,6′-di-[^{1}H]-α-D-galactopyranoside, which are some of the better substrates for GO, are oxidized at the 6-position (*2*). Galactose oxidase can also slowly oxidize the aldehydes produced in the reaction to carboxylic acids (*9*). Galactose oxidase has an unusually broad substrate tolerance for an enzyme, oxidizing a wide variety of primary alcohols to the corresponding aldehydes (*2*); this property makes it useful in a variety of bioanalytical applications (*8*).

Although the catalytic reaction involves a two-electron oxidation of galactose, the presence of a free radical in the active site suggests a homolytic radical hydrogen transfer mechanism for substrate oxidation rather than a mechanism involving heterolytic closed shell hydride transfer chemistry more commonly encountered in oxidative enzymes, such as alcohol dehydrogenase. Previous mechanistic studies have demonstrated that GO stereospecifically abstracts the *pro*-S hydrogen atom from the methylene group alpha to the substrate hydroxyl (*10*), and that there is a substantial kinetic isotope effect with galactose containing deuterium in the 6-methylene position ($k_H/k_D = 7.7$ (for 1-*O*-methyl-6,6′-di-[^{2}H]-β-D-galactopyranoside using a peroxidase-coupled assay)(*10*), 8.7 (from V/K_m measurements for 1-*O*-methyl-6,6′-di-[^{2}H]-α-D-galactopyranoside)(*11*)). Smaller isotope effects (3.1−3.9) have been reported for galactose oxidase turnover using simple β-haloethanols (*12*). The reactions with the β-haloethanols leads to rapid enzyme inactivation by either reduction of the radical center by one electron (reversible) or irreversible halogenation or alkylation of the protein. A solvent isotope effect ($k_{H_2O}/k_{D_2O} = 1.55$) has also been reported for the oxidation of galactose catalyzed by GO (*13*).

Current understanding of the catalytic mechanism of galactose oxidase is based on both structural and biochemical results. The three-dimensional structure of galactose oxidase is now known at high resolution (*14*,*15*). Figure 1 shows the crystallographically determined environment of the catalytic metal center, which includes as ligands a molecule of solvent (H_2O), two histidine imidazoles (H_{496} and H_{581}), and two tyrosinates (Y_{272} and Y_{495}). These are arranged in approximately square pyramidal coordination with Y_{495} at the apex. Crystallographic analyses have revealed a unique thioether bridge between the 3-position of the Tyr-272 ring and Cys-228. This modified tyrosine has been shown to be the site of the stable protein free radical that was characterized in earlier spectroscopic studies (*7*,*16*). On the basis of these findings, a mechanism has been proposed involving free-radical chemistry in the active site (*1*,*17*). The present experiments were designed to test and refine the understanding of the mechanism of this interesting free-radical enzyme.

MATERIALS AND METHODS

Galactose oxidase (E.C. 1.1.3.9) was purified from *Dactylium dendroides* (ATCC 46032) cultures (identical to the *Fusarium spp.* strain NRRL 2903) as previously described (*7*) and converted to the catalytically active form (AGO) by oxidation with 50 mM $K_3Fe(CN)_6$, followed by desalting over a Bio Rad Laboratories BioGel P-30 column equilibrated with 50 mM sodium phosphate buffer, pH 7 (*7*). All spectroscopic and kinetic measurements were performed on protein samples prepared in 50 mM sodium phosphate buffer, pH 7. For kinetic experiments, the buffers were prepared by weighing the components and dissolving them in known volumes of H_2O or D_2O. Protein concentration was determined by optical absorption measurements, using the previously reported molar extinction coefficient [$\epsilon_{280} = 1.05 \times 10^5$ M^{-1} cm^{-1} (*18*)]. The pH dependence of the optical absorption spectrum of the active enzyme was investigated by diluting AGO in sodium phosphate buffer, recording the absorption spectrum, and measuring the pH of the protein solution with a calibrated Beckman combination electrode. The stability of the active enzyme was determined by incubating a 0.1 mM protein solution in a quartz optical cuvette, sealed to prevent evaporation of the solvent. Optical absorption spectra were recorded on a Varian Cary 5 UV−vis−NIR absorption spectrometer interfaced with a PC for data acquisition. All reagents for preparation of culture media and buffers were from commercial sources and were used without purification.

Isotopic substrates were synthesized by modification of previously reported procedures (*19*,*20*). Commercial galacturonic acid (25 g, 0.12 mol) was converted to a mixture of α- and β-anomers of 1,6-dimethyl-D-galacturonate ester by refluxing for 24 h in anhydrous methanol (1.25 L) with methanol-washed Dowex 50 × 2-400 (25 g, H^+ form) as a catalyst (*19*). The α-anomer crystallizes first from concentrated solution. This product was isolated, recrystallized from ethanol, and characterized by elemental analysis (Galbraith Laboratories, Knoxville, TN) (calcd. for $C_8H_{14}O_7$ C: 40.00%, H:6.70%; found: C: 39.95%, H:6.79%) and ^{1}H NMR (300 MHz, D_2O, δ): 3.27 (s, 3H, $-OCH_3$), 3.66 (s, 3H, $-OCH_3$), 3.71 (m, 1H, C−H), 3.79 (d, 1H, C−H), 4.18 (m, 1H, C−H), 4.50 (d, 1H, C−H), 4.76 (d, 1H, C−H). 1-*O*-Methyl-6,6′-di-[^{2}H]-α-D-galactopyranoside was prepared by reduction of 1,6-dimethyl galacturonate (1.0 g, 0.0042 mol) by slow addition of a solution of [^{2}H]-$NaBH_4$ (98 atom % ^{2}H) (0.5 g, 0.012 mol) to the ester in 10 mL water (*20*). After being stirred for 10 min, the mixture was acidified to pH 3−4 by dropwise addition of approximately 50 mL of 1 M acetic acid, and was then purified by passing the reaction mixture over a column (2.5 × 16 cm) containing Bio-Rad Laboratories AG 501-X8(D) mixed bed ion-exchange resin. The deuterated substrate was recrystallized from ethanol. The monohydrate product was characterized by elemental analysis with both ^{1}H and ^{2}H evaluated as ^{1}H (calcd. for $C_7H_{14}O_7$ C: 39.25%, H 7.48%; found C: 39.24%, H 7.74%) and ^{1}H NMR (300 MHz, D_2O, δ): 3.23 (s, 3H, $-OCH_3$), 3.65 (d, 1H, C−H), 3.72 (s, 1H, C−H), 3.79 (d, 1H, C−H), 4.68 (d, 1H,

C−H). The ^{1}H NMR analysis and comparison with authentic 1-*O*-methyl-6,6′-di-[^{1}H]-α-D-galactopyranoside confirmed the identity and anomeric purity of the product.

Rapid kinetics measurements were performed using a Kinetic Instruments Rapid Mixing Spectrophotometer with circulating water bath temperature control. All stopped flow measurements were carried out at 4 °C. Glassware used in handling enzyme samples was washed with hexane, scoured with hot nitric acid, and rinsed with distilled water to remove impurities that can reductively inactivate the enzyme. Galactose oxidase was diluted fresh daily from samples stored at 77 K, transferred to a glass tonometer, and made anaerobic by pump/purge cycling with O_2-free Ar before filling the drive syringes of the rapid mixing spectrophotometer. Substrate solutions prepared in 10 mL syringes were made anaerobic by bubbling with Ar gas pretreated with an Oxiclear O_2 scrubbing cartridge (Labclear, Oakland, CA). Enzyme-monitored turnover reactions were performed using sample buffer equilibrated with pure O_2 gas mixed with anaerobic enzyme. Reactions in D_2O were set up using enzyme and substrates dissolved in D_2O buffer. Data were recorded and analyzed using the DOS-based Program A designed by Rong Chang, Chung-Jeu Chiu, and David Ballou, University of Michigan. Analysis is based on the Marquardt algorithm for solving differential equations (*21*,-*22*). Fits to enzyme-monitored turnover reactions were carried out using Scientist from MicroMath, Salt Lake City, UT.

Steady-state kinetic measurements were performed using a YSI (Yellow Springs, OH) Clark oxygen electrode and a high-accuracy oxygen polarograph circuit (*23*). The temperature of the reaction mixture was controlled by a circulating water bath connected to the water-jacketed reaction chamber. Atmosphere was excluded from the reaction by a standard taper ground glass plug. A calibrated gas mixture (5.09% O_2 in N_2) was obtained from Matheson Gas Products. The concentration of dissolved O_2 in solutions equilibrated with calibrated gas mixtures was calculated according to standard methods (*24*). For measurement of oxygen uptake kinetics at reduced O_2 concentrations, the buffers, wash solutions, and substrates were equilibrated by bubbling with the calibrated gas mixture, which was previously hydrated by sparging through water in a bubbling tower. To standardize the reaction conditions and to help maintain fully active enzyme, 1 mM $K_3Fe(CN)_6$ was routinely included as a component of the assay mixture. Variation of oxygraph performance with changing reaction rates at low temperature was minimized by adjusting the enzyme concentration in the reactions to give approximately uniform rates for both protio- and deutero- substrates. The response of the Clark electrode was calibrated for absolute rate measurements by measuring the amplitude of the oxygen uptake signal in the protocatechuate dioxygenase-catalyzed reaction of aliquot quantities of protocatechuic acid. Protocatechuate dioxygenase was prepared from *Pseudomonas cepacia* DB01 as described by Bull and Ballou (*25*).

RESULTS

Stability of the Active Enzyme. The intense absorption spectra of the active enzyme are virtually unchanged between pH 5.6 and 7.3 in 50 mM sodium phosphate buffer solutions, aside from a slight sharpening of the 445 nm absorption band at lower pH. On prolonged standing, the optical spectra progressively lose intensity as a result of loss of the active site radical. Figure 2 (inset) illustrates the kinetics of decay of the radical in active galactose oxidase in an optical cuvette followed by monitoring the intense visible absorption bands (ϵ_{445}[active enzyme] = 1.0×10^4 M^{-1} cm^{-1}) (Figure 2, spectrum A) associated with the presence of the radical in the protein complex. The decrease in A_{445} at room temperature is consistent with effective first-order decay of the active enzyme, d[AGO]/d$t = -k_1$[AGO] with a rate constant $k_1 = 0.004$ h^{-1}. Thus the predicted half-life for the active enzyme in 50 mM sodium phosphate buffer, pH 7, is approximately one week ($t_{1/2} = 7.2$ d) at ambient temperature in the absence of exogenous reductants.

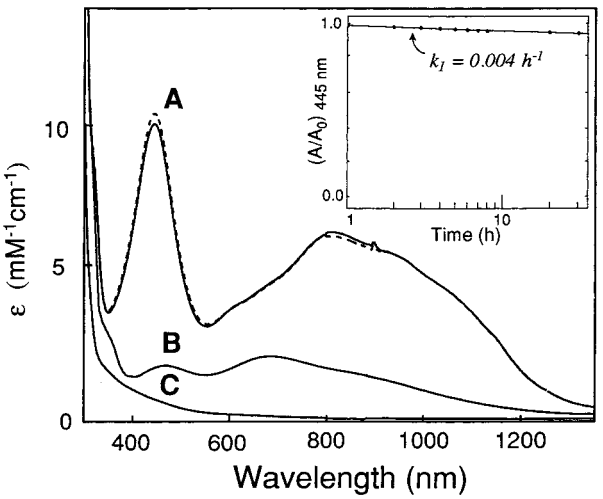

FIGURE 2: Optical spectra of galactose oxidase species and stability of the active enzyme. Galactose oxidase (70 μM) in 50 mM sodium phosphate buffer, pH 7, unless otherwise noted. (A) Redox-activated enzyme (- - -) in 50 mM sodium phosphate buffer, pH 5.6, (—) in 50 mM sodium phosphate buffer, pH 7.3. (B) One-electron reduced inactive enzyme. (C) Substrate-reduced anaerobic enzyme, prepared by addition of a slight excess of 1-*O*-methyl-β-D-galactopyranoside to active enzyme under argon. The extinction coefficients shown are based on the fraction of catalytically competent enzyme (See Discussion). Inset: Fraction of active enzyme (in 50 mM sodium phosphate buffer, pH 7) as a function of time indicated by A_{445}.

Anaerobic Reduction of the Active Enzyme. Although the isolated radical-containing enzyme is remarkably stable in the absence of adventitious reductants, a variety of redox-active small molecules [including hydroxyl-containing buffers such as tris(hydroxymethyl)aminomethane (Tris) and *N*-(2-hydroxyethyl)piperazine-*N*′-2-ethanesulfonate (HEPES)] will reduce the active site, quenching the radical by one-electron reduction (Figure 2, spectrum B). In contrast, hydroxylic compounds that can serve as substrates reduce the enzyme in a two-electron process in the absence of oxygen, converting the active site to the colorless Cu(I) form (Figure 2, spectrum C). We have found that even stopcock grease, or impurities therein, can slowly reduce the enzyme to the inactive form.

The reaction with 1-*O*-methyl-α-D-galactopyranoside is very fast and can be followed by rapid reaction techniques at low temperature (Figure 3; note that the time scale is logarithmic). Anaerobic reduction of the active enzyme by substrate results primarily in a simple exponential relaxation from active to reduced forms, and >95% of the full

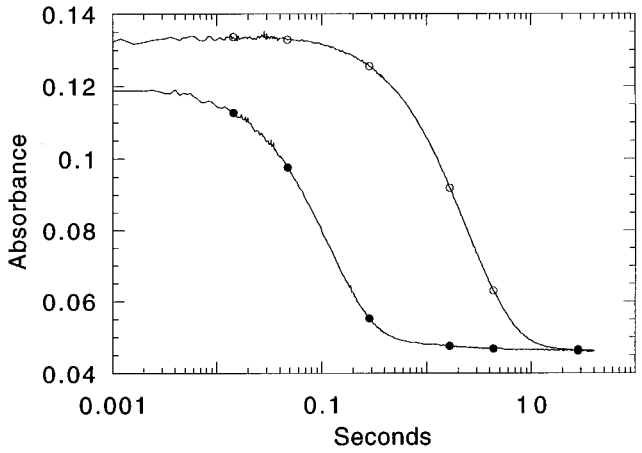

FIGURE 3: Reduction of active galactose oxidase by substrate. Anaerobic AGO was mixed with anaerobic substrate (0.5 mM $[H_2]$-gal or $[D_2]$-gal) in the stopped flow spectrophotometer thermostated at 4 °C and the reaction was monitored at 445 nm. Buffer was 50 mM sodium phosphate, pH 7. The concentration of AGO (after mixing) was 9.4 μM in the $[D_2]$-gal experiment (○) and 7.7 μM in the $[H_2]$-gal experiment (●).

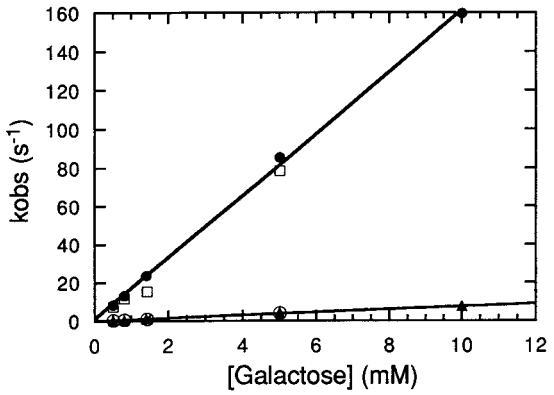

FIGURE 4: Dependence of the observed rate of reduction on substrate concentration for $[H_2]$-gal and $[D_2]$-gal in H_2O and D_2O. Observed rate constants for $[H_2]$-gal (open squares, H_2O; filled circles, D_2O) or $[D_2]$-gal (open circles, H_2O; filled triangles, D_2O).

amplitude of the visible absorption change at 445 nm is associated with the reaction. Two exponentials are required to accurately fit the entire timecourses, but the amplitudes associated with the second phases are relatively small (typically about 5% of the total amplitude at 445 nm) with relatively slow decay kinetics (k_2 less than 10% of k_{red}) and appear to reflect a minor component of the sample. Typical reaction timecourses are displayed in Figure 3 for reactions with 0.5 mM of either 1-*O*-methyl-6,6′-di-[^{1}H]-α-D-galactopyranoside ($[H_2]$-gal) or 1-*O*-methyl-6,6′-di-[^{2}H]-α-D-galactopyranoside ($[D_2]$-gal) substrates with D_2O as the solvent. The use of pyranoside substrates rather than the simple sugars avoids complications from anomeric equilibria in the reactions.

The difference in rates associated with protio versus deutero substrates is emphasized dramatically in Figure 4, where the observed rate constants for reduction of the active site (obtained as described above) are plotted as a function of the concentration of $[H_2/D_2]$-gal. These plots appear second order, because the $[H_2/D_2]$-gal concentrations are $\ll K_d \approx 200$ mM (see below). The calculated second-order rate constants and their ratios (KIE) are given in Table 1. At higher temperatures the reaction with $[H_2]$-gal becomes too fast to accurately measure, even in the stopped-flow spectophotometer. Further analysis of the reaction of deuterated substrate over a wider range of concentrations (0.5−200 mM) shows that the reduction step is saturable with a dissociation constant (K_d) of 180 ± 20 mM for the formation of the initial complex (data not shown).

Table 1: Observed Rate Constants and KIE for Reaction of AGO with $[H_2/D_2]$-gal[a]

solvent	k_H (M^{-1} s^{-1}) (× 10^{-4})	k_D (M^{-1} s^{-1}) (× 10^{-2})	k_H/k_D
H_2O	1.58	7.49	21.1
D_2O	1.60	7.52	21.3

[a] Reactions were carried out as described in the legend to Figure 3, and rate constants were calculated as described in the text.

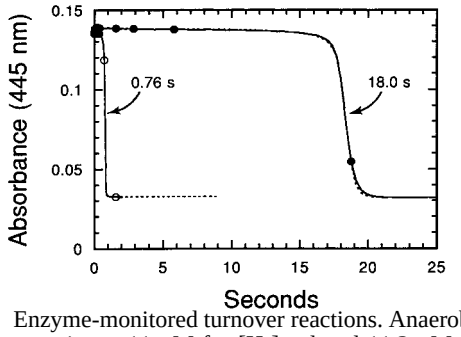

FIGURE 5: Enzyme-monitored turnover reactions. Anaerobic AGO (final concentrations: 11 μM for $[H_2]$-gal and 11.2 μM for $[D_2]$-gal) was mixed with 5 mM $[H_2]$-gal (open circles) or 5 mM $[D_2]$-gal (filled circles) in 50 mM sodium phosphate buffer with D_2O as solvent at 4 °C. Fits (see Discussion) to eqs 5 and 6 using the parameters in Table 2 are plotted as dotted lines.

Since protons are likely to be involved in various steps of the mechanism, we determined the effect of replacing the solvent with D_2O in a parallel series of experiments. These yielded results nearly identical to those found for the reaction in H_2O (Figure 4, Table 1), with a substrate deuterium isotope effect (k_H/k_D) = 21.3 ± 2.5 in D_2O at 4 °C and a negligible normal solvent isotope (k_{H_2O}/k_{D_2O} = 0.99 ± 0.05) for the reaction. Thus there is no evidence for exchangeable protons being involved in any rate-determining step of the reductive half-reaction.

Enzyme-Monitored Turnover (26). To complement the transient state redox kinetics described above and obtain some measure of the oxygen kinetics, steady-state turnover kinetics were performed by mixing the anaerobic enzyme with substrate prepared in O_2-containing buffer. Under the reaction conditions used in this experiment (5 mM galactopyranoside-reducing substrate and 0.58 mM O_2 after mixing), dioxygen stoichiometrically limits the number of catalytic turnovers, while the reducing substrate limits the catalytic rate. In this case, catalysis will proceed at a rate primarily determined by the kinetically limiting substrate until the stoichiometrically limiting component (in this case O_2) is exhausted. This endpoint is signaled when the active enzyme is reduced by the excess alcohol and loss of visible absorption occurs as shown in Figure 5. The number of turnovers until O_2 is exhausted is the same for both $[H_2]$-gal and $[D_2]$-gal, and therefore the time to reach the endpoint of the reaction reflects directly the turnover time for protio and deutero substrates. The durations of the reactions at 4 °C in D_2O were 0.76 s for $[H_2]$-gal using 11 μM AGO, and 18.0 s for $[D_2]$-gal using 11.2 μM AGO (Figure 5). The ratio of these times, corrected for AGO concentration, is 24.1. A similar

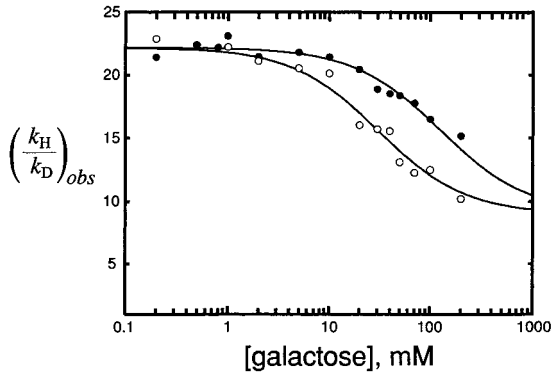

FIGURE 6: Dependence of the isotope effect in galactose oxidase steady-state kinetics on substrate concentration. Absolute rates measured by oxygen uptake using [H_2]-gal or [D_2]-gal substrate were used to evaluate an effective kinetic isotope effect $(k_H/k_D)_{obs}$ for the steady-state reaction over a range of substrate concentrations. Buffer was 50 mM sodium phosphate, pH 7.0, 4 °C. Reactions were performed at both atmospheric [20.9%, 360 μM O_2 (●)] and reduced (5.09%, 88 μM O_2 (○)) oxygen concentrations. Oxygen was equilibrated with buffer solutions at 4 °C. The results are shown together with fits to kinetic rate equations with parameters $k_{red,H} = 1.5 \times 10^4$ M^{-1} s^{-1}, $(k_H/k_D)_{red} = 22$; $k_{ox,H} = 5.1 \times 10^6$ M^{-1} s^{-1}, $(k_H/k_D)_{ox} = 8.5$.

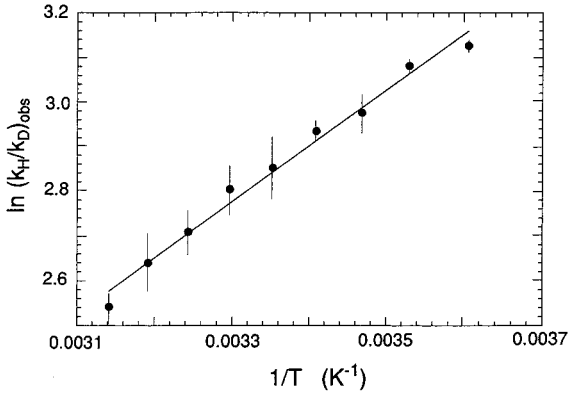

FIGURE 7: Temperature dependence of the isotope effect. Reactions were performed using a thermostated oxygen electrode with solutions equilibrated with atmosphere. All reactions were in 50 mM sodium phosphate buffer (pH 7), with final concentration of AGO being 41 nM for [H_2]-gal and 810 nM for [D_2]-gal. The linear regression fit to the data is also shown.

analysis using H_2O as solvent gives a ratio of 23.8. This number, even with the uncertainty associated with choosing an end point, is very close to the KIE values determined from the analysis of the anaerobic reduction reactions. The fact that GO is essentially fully oxidized during turnover indicates that the reduction of the enzyme by substrate is almost entirely rate-limiting in this turnover experiment. It is clear from these experiments that no solvent isotope effect can be discerned.

Isotope Effects on Steady-State Kinetics. At limiting low and high substrate concentrations, the enzyme-monitored turnover experiments become progressively less accurate and alternative approaches are required to measure the kinetics. Oxygen uptake measurements have been performed under conditions closely paralleling the transient-state reactions, allowing direct comparison between the results of these experiments. A small amount of inorganic oxidant (1 mM $K_3Fe(CN)_6$) was included in these reactions to ensure maintenance of the enzyme in the fully active form. Hamilton and colleagues (*27*) have shown that at this concentration the reduction of O_2 is 4 orders of magnitude faster than reduction of ferricyanide; therefore, the observed oxygen uptake rate is not likely to be affected by inclusion of ferricyanide. Substrate kinetic isotope effects (KIE) $(k_H/k_D)_{obs}$, measured with an oxygen electrode, vary with the substrate concentration as shown in Figure 6. At low substrate concentrations where the reduction step is clearly rate determining in catalysis, the KIE approaches 22.5, but at higher substrate concentrations the KIE decreases significantly to a value near 8. The observed KIE is also sensitive to the amount of dissolved O_2 present. Figure 6 shows that at higher oxygen concentration the curve is displaced to the right. When [H_2/D_2]-gal concentrations are at K_m (≈200 mM) or higher, the reaction with oxygen becomes (partly) rate-limiting. It can be seen that at such high galactose concentrations, where reoxidation by O_2 is kinetically rate-limiting, a significant KIE (≈8) remains, suggesting that there is also a strong primary KIE on the oxygen half-reaction. If true, the hydrogen giving rise to the KIE of 22 in the reductive half-reaction must also particpate in a kinetically significant step in the reaction with oxygen. At concentrations used in these studies, which are mostly below the K_m values for either of the substrates, the point at which crossover for the rate-determining step changes from reduction to oxidation depends on the concentration of both substrates.

Temperature Dependence of the Isotope Effect. To test whether the KIE depends on temperature, the steady-state kinetic parameters were determined at low galactose concentration (1 mM) over the temperature range 4−45 °C measuring the oxygen uptake rate. The KIE was 22.5 at 4 °C and decreased to approximately 13 at 45 °C (Figure 7).

DISCUSSION

Earlier studies (*1*,*7*) have shown that galactose oxidase occurs in three distinct redox states: (1) a redox activated form (AGO) containing a free-radical−Cu(II) complex that gives rise to intense absorption bands in visible−near−IR spectra; (2) a catalytically inactive form (IAGO) containing Cu(II), but no radical; and (3) an O_2-reactive form that is reduced at both the radical site and the metal center and which therefore lacks any significant visible absorption features. Under anaerobic conditions, the reduced enzyme can be prepared by successive one-electron steps from the redox-activated AGO complex or directly by two-electron reduction by reaction with substrates as shown in eq 2,

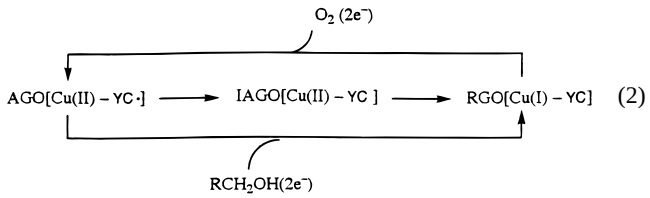

(2)

where YC represents the cross-linked Y_{272}-C_{228} tyrosine-cysteine protein redox site. Distinct optical absorption spectra associated with these species (Figure 2) provide information on the active site structure and interactions in each of these forms. In particular, Y_{495} phenolate coordination to the Cu(II) metal center can be monitored by the presence of the low-energy NIR absorption feature near 900

nm in the active enzyme [assigned to ligand-to-ligand charge transfer (LLCT) absorption in the radical complex (*28*)] and the 450 nm absorption band in the inactive enzyme [arising from phenolate-to-Cu(II) ligand-to-metal charge-transfer absorption (LMCT) (*17*)]. The lack of pH sensitivity of the active enzyme spectrum between pH 5.6 and 7.3 demonstrates the unusual stability of the Cu(II)−phenolate coordination in this complex. The active site phenolate thus appears to be essentially uncoupled from bulk solution proton equilibria. A recent report that the active site of AGO titrates with a pK_a of 6.7 (*29*) may be the result of interactions with hydroxylic buffers and anions.

The absorptivities shown in Figure 2 are based on the concentration of catalytically competent active sites rather than, as previously reported (*7*), on the protein concentration. This accounts for a molar absorptivity of AGO at 445 nm being 10 mM^{-1} cm^{-1}, whereas previously, a value of 5.5 mM^{-1} cm^{-1} has been reported (*7*). The values shown in Figure 2 are based on metal analysis and quantitative EPR spectroscopy of the redox-activated protein as previously described (*7*). Consistent with this, we have determined a value of 10.3 mM^{-1} cm^{-1} from enzyme-monitored turnover experiments using the substrate stoichiometry as a calibration (see below). These results support the conclusion that a significant fraction of activated AGO is depleted in copper and does not contribute to either catalytic activity or visible absorption (*7*).

The native enzyme as isolated is a mixture of active and inactive forms that may be converted nearly quantitatively to the radical-containing active state by treatment with mild oxidants such as ferricyanide (*7*). The protein free radical in this active complex is remarkably stable (Figure 2, inset), quite distinct from transient biological radicals typically generated by radiolysis or oxidative damage. The only other protein radical of comparable stability is the noncatalytic tyrosine free radical in ribonucleotide reductase (*30,31*), whose stability is attributed to its isolation in the hydrophobic core of the protein. In contrast, the radical site in galactose oxidase lies in the active site close to the protein surface (*14,15*), making its stability all the more remarkable. Previous reports of autoredox instability of the active enzyme (*29*) likely relate to reactions with buffer or with small quantities of reducing impurities in the sample preparation that serve as inactivators or as substrates. The reduction experiment (Figures 3 and 4) required scrupulous care in removing (or oxidizing) reducing substances on the glassware and in the stopped-flow spectrophotometer.

The stability of the redox activated enzyme species has permitted us to investigate the transient state anaerobic substrate reduction reaction under conditions in which both O_2 and adventitious reductants are excluded (Figures 3 and 4). This reaction represents half of the catalytic turnover cycle and can be studied separately from the reaction of the reduced enzyme with dioxygen. The results obtained here lead to a description of the reaction of active galactose oxidase (AGO) with reducing substrate (alcohol or aldehyde, S) leading to product (aldehyde or carboxylate, P) in a process that involves initial formation of a weak collision complex within which redox occurs (eq 3):

$$\mathrm{AGO} + \mathrm{S} \overset{K_d}{\rightleftarrows} \{\mathrm{AGO{-}S}\} \overset{k_1}{\rightarrow} \mathrm{RGO{-}P} \qquad (3)$$

The K_d determined for the anaerobic substrate reduction step (180 mM with [D_2]-gal) is comparable to the Michaelis constant for 1-*O*-methyl-β-D-galactopyranoside derived from steady-state kinetic analysis (K_m = 175 mM at saturating concentration of O_2)(*32*); this indicates that at the lower concentrations of [H_2/D_2]-gal used in these experiments, the reaction behaves essentially bimolecularly. The low affinity for substrate is consistent with the well-known lack of substrate selectivity exhibited by this enzyme, which may imply a tradeoff in the design of the active site for catalytic speed at the expense of selectivity, or may simply reflect the possibility that H_2O_2 is the biologically important product and that it is advantageous to be able to use a variety of reducing substrates as a generic source of hydrogen.

Recent enzyme-monitored turnover kinetics studies on galactose oxidase (*29*) have reported kinetic constants somewhat different from those found here. In particular, a reduction rate constant of $k_{red} = 1.2 \times 10^4$ M^{-1} s^{-1} (25 °C) was reported (*29*), which is somewhat lower than the value 1.5×10^4 M^{-1} s^{-1} (4 °C) found in our transient reduction experiments. A normal Arrhenius factor for the temperature dependence would predict an approximately 4-fold greater rate at the higher temperature. The results can, however, be partially reconciled by examining the assumptions on which these values are based. Our transient kinetics measurement of k_{red} is independent of the amount of enzyme present, and therefore does not depend on knowing the molar absorptivity of the active enzyme. In contrast, evaluation of k_{red} from the enzyme-monitored turnover experiment requires accurate knowledge of the amount of active enzyme in the sample. The total absorption change ($\Delta A_{450} = 0.025$) reported in the earlier study was interpreted in terms of reducing 8.7 μM of active galactose oxidase. Using the correct $\Delta\epsilon = 9450$ M^{-1} cm^{-1} for reduction of AGO (Figure 2) indicates that the actual concentration of active enzyme was only 2.6 μM, yielding a revised estimate of $k_{red} = 4 \times 10^4$ M^{-1} s^{-1} (25 °C) which is close to the expected value (6×10^4 M^{-1} s^{-1}).

We have used enzyme-monitored turnover experiments (Figure 5) to explore the kinetic isotope effects in the steady-state turnover reaction. The experimental reaction traces for 5 mM [H_2]-gal and [D_2]-gal in D_2O are shown in Figure 5. Initially, the absorbance traces indicate that during turnover the enzyme is nearly fully oxidized, implying that even though the reaction with substrate is very fast, the reaction with O_2 is at least an order of magnitude faster, making the reducing substrate almost completely rate-limiting for turnover. Thus the time required to complete a single catalytic turnover cycle is equal to the reciprocal of the reduction rate constant (k_{obs}) at a given concentration of reducing substrate (for 5 mM galactose in D_2O, $k_H^{-1} = 0.0125$ s; $k_D^{-1} = 0.266$ s). Since [H_2]-gal is greatly in excess and can be considered nearly constant during the turnover, the duration (T) of the turnover is determined by the number of catalytic cycles required to exhaust the stoichiometrically limiting substrate (O_2). This can be calculated from eq 4 where [E] is the concentration of active enzyme:

$$T = \left(\frac{[\mathrm{O_2}]}{[\mathrm{E}]}\right) {k_{obs}}^{-1} \qquad (4)$$

Table 2: Fitted Parameters for Figure 5[a]

parameter	$[H_2]$-gal	$[D_2]$-gal	KIE
k_{red}	1.53×10^4 M^{-1} s^{-1}	6.3×10^2 M^{-1} s^{-1}	24.3
k_{ox}	7.99×10^6 M^{-1} s^{-1}	1.02×10^6 M^{-1} s^{-1}	7.8
$\epsilon_{ox,445}$	10.3 mM^{-1} cm^{-1}	10.3 mM^{-1} cm^{-1}	
$\epsilon_{red,445}$	0.8 mM^{-1} cm^{-1}	0.8 mM^{-1} cm^{-1}	

[a] See text for description of how values were determined.

For 11 μM active galactose oxidase and 585 μM O_2, 53 turnover reaction cycles are required to completely consume the dissolved oxygen, after which the enzyme becomes reduced and bleaches. Neglecting the change in the reaction rate as both $[H_2]$-gal and $[O_2]$ decrease (especially as $[O_2]$ becomes low), as well as any loss of activity during turnover, the duration of the steady-state turnover phase is predicted to be 0.67 s, in reasonable agreement with the observed value of 0.76 s. Similarly, based on the anaerobic reduction rate constant for the deuterated $[D_2]$-gal substrate, a duration of 14 s is predicted for the turnover phase compared to the 18 s observed. The ratio, (18 s)/(0.76 s) gives an apparent full KIE ($k_H/k_D = 24$) from these enzyme-monitored turnover measurements at 5 mM substrate. This suggests that under physiological conditions substrate oxidation is rate-limiting in turnover.

We also fit the data in Figure 5 to eqs 5 and 6 using the program, Scientist, and the appropriate differential equations.

$$E_{ox} + S \xrightarrow{k_{red}} E_{red} + P \quad (5)$$

$$E_{red} + O_2 \xrightarrow{k_{ox}} E_{ox} + H_2O_2 \quad (6)$$

E_{ox} and S at $t = 0$ were fixed as described in the legend to Figure 5. Parameters fitted are k_{red}, k_{ox}, $\epsilon_{ox,445}$, and $\epsilon_{red,445}$ in the $[H_2]$-gal experiment. For analysis of the $[D_2]$-gal experiment, the values of $\epsilon_{ox,445}$ and $\epsilon_{red,445}$ were fixed to those determined in the $[H_2]$-gal fits. The fits are indicated in Figure 5 as dotted lines, and they demonstrate that the assumption of a bimolecular approximation at substrate concentrations well below K_m is quite reasonable. The fitted parameters (Table 2) are in remarkable agreement with both the reduction studies and the oxygen uptake studies (see below). In addition, they are in accord with the corrected absorptivity of the active site as shown in Figure 2 and discussed above. Using the lower, protein-based absorptivity values, we would have calculated a higher enzyme concentration in these experiments; the fits would then have yielded a correspondingly smaller k_{red}, in conflict with the reduction studies.

Oxygen uptake studies have also allowed us to detect the kinetic isotope effects for both the reductive and the oxidative half-reactions. The most obvious feature of the data from oxygraph measurements (Figure 6) is the strong dependence of KIE on substrate concentration, a characteristic not observed for the isolated anaerobic reduction reaction. The sensitivity to substrate concentration can be understood in terms of a ping-pong kinetic mechanism for AGO. The overall rate depends on both half-reactions, with reduction of AGO being limiting at low concentration of [H/D]-gal, and oxidation by O_2 being limiting at high concentrations of the reducing substrate. The dependence of the KIE on substrate (S) and O_2 can be predicted from the reciprocal rate eqs 7 and 8:

$$(k_H)^{-1}_{obs} = (k_{red,H}[S])^{-1} + (k_{ox,H}[O_2])^{-1} \quad (7)$$

$$(k_D)^{-1}_{obs} = (k_{red,D}[S])^{-1} + (k_{ox,D}[O_2])^{-1} \quad (8)$$

Dividing eq 8 by eq 7 and rearranging gives an expression for the effective isotope effect:

$$(k_H/k_D)_{obs} = \frac{(k_H/k_D)_{red}}{\left(1 + \left(\frac{(k_{red,H}[S])}{(k_{ox,H}[O_2])}\right)\right)} + \frac{(k_H/k_D)_{ox}}{\left(1 + \left(\frac{(k_{ox,H}[O_2])}{(k_{red,H}[S])}\right)\right)} \quad (9)$$

Accordingly, at low substrate concentration, where substrate oxidation is rate-limiting, the experimentally determined $(k_H/k_D)_{obs}$ should approach the full value of the kinetic isotope effect expressed in the anaerobic substrate reduction reaction, $(k_H/k_D)_{red}$. Conversely, at high $[H_2/D_2]$-gal concentration, where dioxygen reduction becomes rate-limiting, the measured value of $(k_H/k_D)_{obs}$ should reflect the kinetic isotope effect for the O_2 half-reaction, $(k_H/k_D)_{ox}$. Figure 6 shows that this value approaches a value of about 8 at "infinite" reducing substrate, implying a significant KIE on the O_2 half-reaction. A similar value was obtained previously from steady-state kinetic analysis with extrapolation to infinite [S]; this KIE was attributed at that time to substrate oxidation (*11*). The observed KIE on the oxygen reaction, coupled with the determinations of the KIE extrapolated to infinite substrate concentrations by Villafranca et al. (11), suggests that at infinite concentrations of both substrates the overall rate of catalysis is limited by the transfer of the hydrogen from tyrosine-272 (originally the *pro*-S hydrogen of the substrate) to oxygen rather than transfer from galactose to tyrosine-272. At concentrations of galactose normally encountered (which are well below K_m values), the very high apparent second-order reaction of oxygen masks the isotope effect on the oxidative half-reaction and the KIE of 22 for the reduction reaction is observed.

The transition between these two limiting values of KIE occurs within a substrate concentration range that depends on the relative rates of each of the four reactions (substrate oxidation and O_2 reduction with both protio and deutero substrates). The oxygen half-reaction becomes rate-limiting at lower substrate concentrations for the ^{1}H-galactopyranoside than for the corresponding ^{2}H derivative, resulting in the characteristic behavior shown in Figure 6. Equation 9 predicts that the transition range will be shifted to lower substrate concentrations at reduced oxygen concentrations. As shown in Figure 6, this behavior is observed experimentally, with the transition curve for solution equilibrated with 5% O_2 (88 μM) lying below the curve for equilibration with atmospheric oxygen (approximately 21% or 360 μM at 4 °C). Knowing the apparent second-order substrate reduction rate constant from both anaerobic transient reaction kinetics and calibrated oxygraph turnover kinetics, as well as the concentration of dissolved oxygen computed according to standard methods, the value of k_{ox} and the corresponding KIE for the O_2 half-reaction can be determined by fitting the experimental data to eq 9. We obtain values of $k_{ox,H}$ =

7×10^6 M^{-1} s^{-1} and $(k_H/k_D)_{ox} = 8$, which are consistent with the enzyme-monitored turnover experiments (Table 2) and with the previously reported KIE for this substrate.

The observation of a substrate KIE in both half-reactions implies that the isotope is retained in the active site during catalysis. Based on this interpretation, the absence of any detectable solvent isotope (k_{H_2O}/k_{D_2O}) effect requires that any solvent exchange reaction for protons involved in kinetically significant reactions must be much slower than the reoxidation rate, even at reduced oxygen concentrations. It might be possible, however, to detect a solvent KIE on reoxidation of reduced Cu(I) enzyme that has been fully equilibrated with H_2O or D_2O. Alternatively, the apparent KIE on the oxidative half-reaction may simply result from the relative limiting rates (K_{red} and K_{ox}) of the two half-reactions being similar. In a ping-pong mechanism, the overall limiting rate for protio and deutero substrates is related to the individual half-reaction rates as shown in eqs 10 and 11:

$$(V_{max,H})^{-1} = (K_{red,H})^{-1} + (K_{ox,H})^{-1} \quad (10)$$

$$(V_{max,D})^{-1} = (K_{red,D})^{-1} + (K_{ox,D})^{-1} \quad (11)$$

where $V_{max,H}$ and $V_{max,D}$ are the maximum velocities with protio and deutero substrates, and $K_{red,H} = \text{KIE} \bullet K_{red,D}$, KIE being the full isotope effect measured in the substrate reduction half-reaction with $K_{ox,H} = K_{ox,D}$. The apparent isotope effect extrapolated to infinite concentrations of both substrates will then be given by eq 12:

$$(V_{max,H}/V_{max,D}) = (\text{KIE} \bullet K_{ox,H} + K_{red,H})/(K_{ox,H} + K_{red,H}) \quad (12)$$

If both half-reactions had the same limiting rate K in the presence of protio substrate, one would predict an apparent overall isotope effect half that observed in the isolated substrate reduction step, which is about what we observe. Thus, at this time we cannot distinguish whether our results are due to a KIE on the oxygen reaction or to a serendipitous similarity of the intrinsic oxidation and reduction rates (K_{ox} and K_{red}).

These results lead to a detailed picture of galactose oxidase redox catalysis that is initiated by weak (almost collisional) association with the reducing substrate (Figure 8). The orientation of the bound substrate shown in the figure is consistent with the stereospecific abstraction of the *pro*-S hydrogen (*10*) by the nearby (1.2 Å) Y_{272} phenoxyl radical. Knowles and Ito (*33*) have modeled galactose into the site in a similar manner and have shown that this orientation also accounts reasonably for the substrate selectivity of AGO (i.e., the lack of turnover with isomeric substrates such as D-glucose and L-galactose) as well as for the *pro*-S hydrogen stereospecificity.

Replacing water by alcohol in the axial position of the Cu(II) complex (defined as the direction of weakest ligand interaction) initially results in weak coordination of substrate to the active-site metal ion. Deprotonation of the alcohol strengthens this interaction, stabilizing the complex and activating substrate for oxidation. Y_{495} is within 2.8 Å of the alcoholic proton and is positioned to function as a general base, accepting a proton in the ligand binding process as shown previously (*17*). When the phenolate of Y_{495} abstracts the hydroxylic proton of the coordinated substrate [acidified

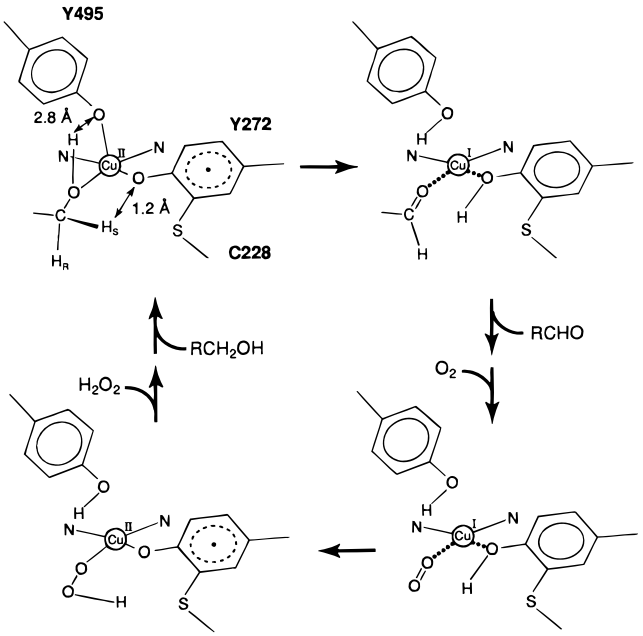

FIGURE 8: Galactose oxidase turnover cycle. The hydroxylic substrate is modeled in the galactose oxidase active site by conservative replacement of crystallographic water in the metal coordination sphere with a primary alcohol in an orientation consistent with stereospecific *pro*-S hydrogen abstraction from the methylene carbon. Predicted hydrogen-bonded distances from the hydroxylic proton to the Y_{495} phenolate oxygen and from the methylene *pro*-S hydrogen to the Y_{272} phenoxyl oxygen are indicated.

by interaction with the Cu(II) Lewis acid (*34*)], a change in ligand interaction occurs giving a new geometry at the metal center. This pseudorotation at copper puts the protonated tyrosine in the weak axial position in the complex (Figure 9, top left). The equatorial alkoxide now interacts strongly with the Cu(II) and has direct covalent interactions with the $d_{x^2-y^2}$ metal redox orbital that projects in the plane of a square pyramidal complex. There are at least two reasonable scenarios for completion of the reduction of the enzyme. The first has electron transfer followed by H-atom transfer (Figure 9, top), and the second has the steps in reverse order (Figure 9, bottom).

In the first proposal, the new coordination geometry permits fast inner sphere electron transfer, reducing the metal ion [Cu(II)→Cu(I)] (Figure 9, top). The ketyl radical generated by this one-electron oxidation would then undergo C−H bond cleavage with hydrogen atom transfer to the phenoxyl oxygen of the cysteinyl-tyrosine radical site, yielding the aldehyde and converting the radical to the singlet modified tyrosine (Figure 9, top). The rate-limiting step in reduction is the H-atom transfer. This mechanism is attractive because the radical character of the enzyme active site is reflected in the radical character of the catalyzed reaction, and the rapid electron transfer is consistent with the fast charge transfer expected for inner sphere processes. However, because bleaching at 445 nm would be expected in the electron transfer step, the only way a significant KIE would be observed by this mechanism is if the electron transfer step significantly favors Cu(II), so that the rate-limiting H-atom transfer would drive the overall reaction to the full reduction of the enzyme. The large KIE (22.5) could thus arise from a combination of factors. The H-atom transfer could have a KIE between 7 and 10. If the electron-

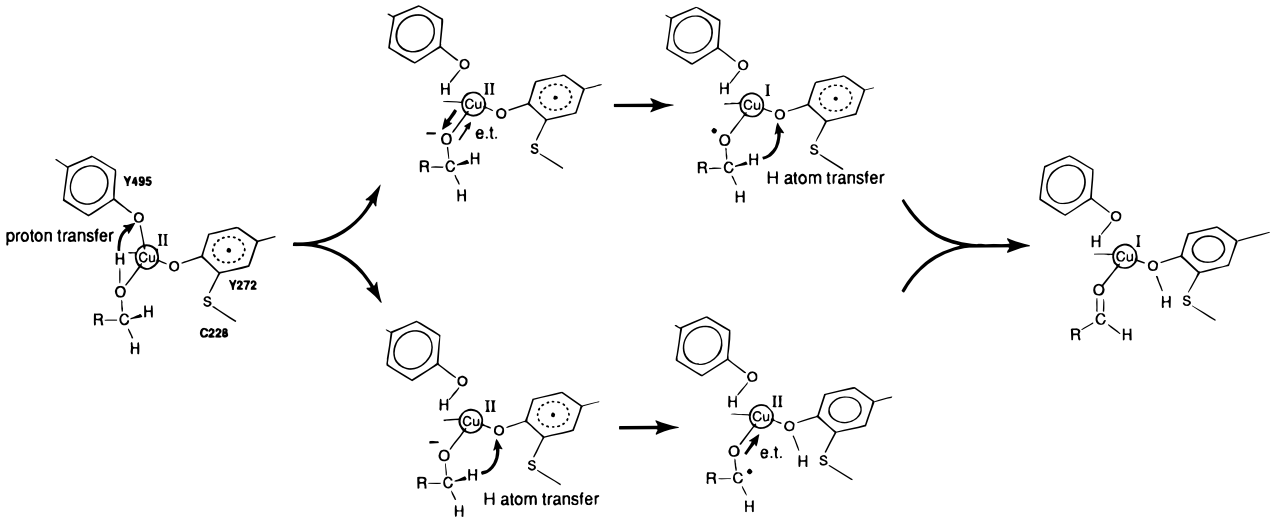

FIGURE 9: Radical mechanism for reduction of the active site of AGO by an alcohol. Three key steps of the proposed radical redox mechanism are illustrated here: proton transfer from coordinated substrate hydroxyl to the Y_{495} phenolate activates the substrate for oxidation chemistry; inner sphere electron-transfer reduces the Cu(II) metal center; hydrogen atom transfer associated with homolytic C−H bond cleavage and reduction of the Y_{272} phenoxyl. The ordering of electron transfer and atom transfer steps are reversed between the top and bottom sequences.

transfer step were to exhibit an equilibrium isotope effect (*35*) arising from the two deuteriums in [D_2]-gal, a fractionation factor of 0.8 would be sufficient to account for the observed KIE of 22.5, since the KIE's of the two steps are multiplicative.

The second possibility has the H-atom transfer occurring first (Figure 9, bottom). In this mechanism, which has been proposed previously (*17*), the bleaching would not occur until the H-atom transfer permitted the very rapid inner sphere reduction of Cu(II). Although this mechanism can easily explain a fully observable isotope effect, accounting for a KIE as large as 22.5 is more difficult. This value is far greater than the theoretical limit defined by the force constants for C−^{1}H and C−^{2}H bond stretching modes ($k_H/k_D = 9$), although it might be consistent with the larger normal deuterium kinetic isotope effect predicted if softening of C−H bending modes also occurs in the transition state ($k_H/k_D = 15-20$) (*36*). Secondary deuterium isotope effects associated with the change in C−H bonding as the carbon undergoes rehybridization ($sp^3 \rightarrow sp^2$) are generally relatively small, typically below 1.4 (*36*) and therefore do not fully explain our observations. The two reactions (electron and hydrogen atom transfer) probably do not occur in a concerted fashion, as previously proposed (*12*), because the redox sites are chemically distinct and the activation barriers are expected to be quite different. Moreover, since the hydroxylic proton of substrate exchanges rapidly in D_2O, the absence of any significant solvent KIE for substrate oxidation mitigates against a concerted proton/hydrogen-atom transfer process. Nevertheless, it is clear that C−H bond cleavage via a radical reaction is fully rate-limiting for substrate oxidation.

Large, nonclassical KIE, such as those found here, have been attributed to tunneling processes, where the different localization of vibrational wave functions for deuterium and hydrogen becomes important (*37*). A strong temperature dependence of the KIE is normally expected for tunneling kinetics (*37*). The studies reported here demonstrate such a strong temperature dependence of KIE and are therefore consistent with a tunneling mechanism. The slope of the temperature dependence plot (Figure 7), equal to $(E_a(D) - E_a(H))/R$, reflects an apparent difference in activation energies for C−H bond cleavage in protio- and deutero-galactose. This is expected because of the different zero-point energies for C−^{1}H and C−^{2}H bonds. However, the strong temperature dependence observed in the experiment (Figure 7) implies a large apparent activation parameter ($E_a(D) - E_a(H)) = 10.4$ kJ/mol, exceeding the semiclassical upper limit (5.8 kJ/mol)(*38*). Similarly, the intercept of the temperature dependence yields an estimate of the ratio of Arrhenius parameters for the protio- and deutero-reactions ($A_H/A_D = 0.25$) lower than the absolute minimum semiclassical lower limit (0.7−0.9)(*39*). These anomalous results are characteristic of processes involving barrier-tunneling contributions to the reaction, resulting in a breakdown of the semiclassical barrier-hopping kinetic theory. The strong temperature dependence of KIE observed in these experiments is therefore consistent with a mechanism for galactose oxidase involving tunneling of a hydrogen atom in the rate-determining step.

Catalytic conversion of the alcohol substrate to aldehyde completes the reductive half-reaction of the turnover cycle, leaving the enzyme in the Cu(I) [RGO] reduced state. This intermediate state, which we have previously characterized both biochemically and structurally (*7,40,41*), is stable in the absence of oxygen and is competent for rapid reaction with O_2 to complete the catalytic cycle (Figure 8). In this state Cu(I) is coordinated by 2−3 ligands, most likely the two histidines, with possible additional weak interactions with the Y_{272} phenol, resulting in T-coordination at copper that is relatively favorable for the univalent Cu(I) oxidation state (*41*). The existence of this stable reduced intermediate has provided strong evidence in support of a ping-pong mechanism for enzyme turnover:

$$\underset{\downarrow}{RCH_2OH} \qquad \underset{\uparrow}{RCHO} \qquad \underset{\downarrow}{O_2} \qquad \underset{\uparrow}{H_2O_2}$$

A ping-pong mechanism for galactose oxidase turnover was originally proposed by Hamilton (*42*), but (at that time) was excluded by reports that the enzyme remains in the Cu-

(II) state in the presence of reducing substrate. This observation is now known to be a consequence of the redox heterogeneity of the native enzyme that leads to a significant amount of EPR-active Cu(II)-containing IAGO species that does not respond to addition of either the reducing substrate or oxygen (*7*). Since neither of the states involved in the substrate redox reaction (the active oxidized nor the fully reduced forms) is detectable by EPR spectroscopy, the catalytic complexes were not observed in these earlier studies. More recently, the ping-pong mechanism has been brought into question by steady-state kinetics studies in which the deuterium isotope effect for galactose substrate was measured over a range of substrate and oxygen concentrations (*11*). In that case, the presence of a kinetic isotope effect associated with the O_2 reaction was interpreted as evidence for a rapid equilibrium ordered mechanism in which both substrates are simultaneously bound in the active site before the hydrogen is transferred. This interpretation is based in part on the reasonable assumption that a substrate KIE will only appear in the half-reaction in which bond cleavage occurs (the oxidation of substrate). If, as our studies suggest, isotope is retained in the active site, it will give rise to an isotope effect in the second half-reaction, which will be observed only when that reaction becomes rate-limiting, at high concentrations of galactose as shown by eq 7. Recent studies by Borman et al. (*29*) also appear to support this ping-pong kinetic mechanism. They carried out kinetic studies of galactose by enzyme-monitored turnover methods (*25*) using five different substrates, each at several pH values. Although k_{red} varied severalfold among the substrates, k_{ox} was 1×10^7 M^{-1} s^{-1} for all determinations. This implies that O_2 reacts with free E_{red} rather than with E_{red}•P as would be required in a ternary complex mechanism.

CONCLUSIONS

The mechanism of substrate oxidation by galactose oxidase has been probed by isotopic perturbation of the turnover reaction. Methylene di-deuterated substrate introduces a dramatic 22-fold KIE on substrate reduction, which is also detected in the oxygen-limited enzyme-monitored turnover reaction at low substrate concentrations. A large KIE of about 8 persists in the O_2 reaction, apparently resulting from retention of isotope that is then involved in the rate-limiting step for formation of H_2O_2. We have presented a scheme involving a radical redox mechanism in which hydrogen atom transfer occurs in the transition state for both substrate oxidation and O_2 reduction half-reactions to account for these experimental results.

ACKNOWLEDGMENT

We thank Dr. Bruce Palfey, University of Michigan, for helpful discussion and assistance with data fitting and Dr. James Peliska, University of Michigan, for helpful discussions.

REFERENCES

1. Whittaker, J. W. (1994) in *Metal Ions in Biological Systems* (Sigel, H., and Sigel, A., Eds.) pp 315−360, Marcel Dekker, Basel.
2. Avigad, G., Amaral, D., Asensio, C., and Horecker, B. L. (1962) *J. Biol. Chem. 237*, 2736−2743.
3. Kosman, D. J. (1985) in *Copper Proteins and Copper Enzymes*, (Lontie, R., Ed.) Vol. 2, pp 1−26, CRC Press, Boca Raton, FL.
4. Kersten, P. J. (1990) *Proc. Natl. Acad. Sci. U.S.A. 87*, 2936−2940.
5. Whittaker, M. M., Kersten, P. J., Nakamura, N., Sanders-Loehr, J., Schweizer, E. S., and Whittaker, J. W. (1996) *J. Biol. Chem. 271*, 681−687.
6. Bork, P., and Doolittle, R. F. (1994) *J. Mol. Biol. 236*, 1277−1282.
7. Whittaker, M. M., and Whittaker, J. W. (1988) *J. Biol. Chem. 263*, 6074−6080.
8. Johnson, J. M., Halsall, H. B., and Heineman, W. R. (1982) *Anal. Chem. 54*, 1394−1399.
9. Kelleher, F. M., and Bhavanadan, V. P. (1986) *J. Biol. Chem. 261*, 11045−11048.
10. Maradufu, A., Cree, G. M., and Perlin, A. S. (1971) *Can. J. Chem. 49*, 3429−3437.
11. Villafranca, J. J., Freeman, J. C., and Kotchevar, A. (1993) in *Bioinorganic Chemistry of Copper* (Karlin, K. D., and Tyeklar, Z., Eds.) pp 439−446, Chapman and Hall, New York.
12. Wachter, R. M., Montague-Smith, M. P., and Branchaud, B. P. (1997) *J. Am. Chem. Soc. 119*, 7743−7749.
13. Driscoll, J. J., and Kosman, D. J. (1987) *Biochemistry 26*, 3429−3436.
14. Ito, N., Phillips, S. E. V., Stevens, C., Ogel, Z. B., McPherson, M. J., Keen, J. N., Yadav, K. D. S., and Knowles, P. F. (1991) *Nature 350*, 87−90.
15. Ito, N., Phillips, S. E. V., Yadav, K. D. S., and Knowles, P. F. (1994) *J. Mol. Biol. 238*, 794−814.
16. Whittaker, M. M., and Whittaker, J. W. (1990) *J. Biol. Chem. 265*, 9610−9613.
17. Whittaker, M. M., and Whittaker, J. W. (1993) *Biophys. J. 64*, 762−772.
18. Kosman, D. J., Ettinger, M. J., Weiner, R. E., and Massaro, E. J. (1974) *Arch. Biochem. Biophys. 165*, 456−467.
19. Bollenback, G. N. (1963) in *Methods in Carbohydrate Chemistry*, (Whistler, R. L., and Wolfrom, M. L., Eds.) Vol. 2, pp 326−328, Academic Press, New York.
20. Lewis, B. A., Smith, F., and Stephen, A. M. (1963) in *Methods in Carbohydrate Chemistry*, (Whistler, R. L., and Wolfrom, M. L., Eds.) Vol. 2, pp 68−76, Academic Press, New York.
21. Bevington, D. R. (1969) *Data Reduction and Error Analysis for the Physical Sciences*, pp 235−249, McGraw-Hill, New York.
22. Press, W. H., Teukolsky, S. A., Vetterling, W. T., and Flannery, B. P. (1992) in *Numerical Recipes in C, the Art of Scientific Computing*, 2nd ed., pp 683−688, Cambridge University Press, New York.
23. Meunier, P. C., and Popovic, R. (1988) *Rev. Sci. Instrum. 59*, 486−491.
24. Hitchman, M. L. (1978) *Measurement of Dissolved Oxygen*, pp 7−33, John Wiley & Sons, York, NY.
25. Bull, C., and Ballou, D. P. (1981) *J. Biol. Chem. 256*, 12673−12680.
26. Gibson, Q. H., Swaboda, B. E. P., and Massey, V. (1964) *J. Biol. Chem. 250*, 4048−4052.
27. Hamilton, G. A., Adolf, P. K., de Jersey, J., DuBois, G. C., Dyrkacz, G. R., and Libby, R. D. (1978) *J. Am. Chem. Soc. 100*, 1899−1912.
28. McGlashen, M. L., Eads, D. D., Spiro, T. G., and Whittaker, J. W. (1995) *J. Phys. Chem. 99*, 4918−4922.
29. Borman, C. D., Saysell, C. G., and Sykes, A. G. (1997) *J. Biol. Inorg. Chem. 2*, 480−487.
30. Sjöberg, B.-M., Reichard, P. Gräslund, A., and Ehrenberg, A. (1978) *J. Biol. Chem. 253*, 6863−6865.
31. Sjöberg, B.-M., and Gräslund, A. (1983) *Adv. Inorg. Biochem. 5*, 87−110.
32. Kwiatkowski, L. D., Adelman, M., Pennelly, R., and Kosman, D. J. (1981) *J. Inorg. Biochem. 14*, 209−222.

33. Knowles, P. F., and Ito, N. (1993) *Perspect. Bioinorg. Chem. 2*, 207−244.
34. Kimura, E., Nakamura, I., Koike, T., Shionoya, M., Kodama, Y., Ikeda, T., and Shiro, M. (1994) *J. Am. Chem. Soc. 116*, 4764−4771.
35. Cleland, W. W. (1980) *Methods Enzymol. 64*, 104−125.
36. Melander, L., and Saunders, W. H., Jr. (1987) *Reaction Rates of Isotopic Molecules*, Krieger Publishing Co., Malabar, FL.
37. Cha, Y., Murray, C. J., and Klinman, J. P. (1989) *Science 243*, 1325−1330.
38. Bell, R. P. (1980) *The Tunnel Effect in Chemistry*, Chapman and Hall, New York.
39. Schneider, M. E., and Stern, H. J. (1972) *J. Am. Chem. Soc. 94*, 1517−1522.
40. Clark, K., Penner-Hahn, J. E., Whittaker, M. M., and Whittaker, J. W. (1990) *J. Am. Chem. Soc. 112*, 6433−6434.
41. Clark, K., Penner-Hahn, J. E., Whittaker, M. M., and Whittaker, J. W. (1994) *Biochemistry 33*, 12553−12557.
42. Hamilton, G. A., de Jersey, J., and Adolf, P. K. (1973) in *Oxidases and Related Redox Systems*, (King, T. E., Mason, H. S., and Morrison, M., Eds.), Vol. 1, pp 103−124, University Park Press, Baltimore, MD.

BI980328T